water

MDPI

Article

Optimal Selection of Sampling Points for Detecting SARS-CoV-2 RNA in Sewer System Using NSGA-II Algorithm

Argyro Gkatzioura * and Antigoni Zafeirakou

Department of Civil Engineering, Aristotle University of Thessaloniki, 54124 Thessaloniki, Greece; azafir@civil.auth.gr

* Correspondence: gargyro@civil.auth.gr

Abstract: Sampling and analysing urban wastewater are found to be a reliable indicator of the regional spread of infectious diseases. During the COVID-19 pandemic, several research groups around the globe sampled wastewater from treatment plants or other points throughout a sewer system and tried to identify the presence of the virus. Since infected persons are found to excrete the virus in their feces and urine, urban wastewater analysis proved to be a valuable tool for the early detection of spikes in the disease. In the present study, an effort was made to investigate several fate and transport scenarios of SARS-CoV-2 in a sewer system. USEPA's Storm Water Management Model (SWMM) was utilized for the analysis. The modelling results were then used as an input to an optimization procedure using an NSGA-II algorithm. The optimization procedure aimed to determine the appropriate number and combination of sampling points for a better assessment of the disease's dispersion in the community. Four to six sampling points seem to offer a high likelihood of SARS-CoV-2 RNA detection in minimum time, representing the maximum population.

Keywords: SARS-CoV-2; EPA SWMM; wastewater; wastewater surveillance; sampling points; optimization; wastewater-based epidemiology

Citation: Gkatzioura, A.; Zafeirakou, A. Optimal Selection of Sampling Points for Detecting SARS-CoV-2 RNA in Sewer System Using NSGA-II Algorithm. *Water* **2023**, *15*, 4076. https://doi.org/10.3390/w15234076

Academic Editor: Christos S. Akratos

Received: 5 October 2023
Revised: 8 November 2023
Accepted: 21 November 2023
Published: 24 November 2023

1. Introduction

Wastewater is normally considered a source of contamination; however, it can also serve as a source of information. It can deliver useful information for several parameters concerning the population living in a certain sewershed; this practice is referred to as wastewater surveillance or wastewater-based epidemiology (WBE). Wastewater analysis can reveal pharmaceuticals' consumption patterns [1,2], the occurrence of antibiotics and development of antibiotic resistance [3,4], human exposure to pesticides [5], and the presence of viruses such as poliovirus [6,7], noroviruses [8], Hepatitis B virus [9], and SARS-CoV [10].

Since the spread of the new coronavirus SARS-CoV-2 worldwide, causing the COVID-19 disease, wastewater surveillance for the presence of SARS-CoV-2 viral RNA has become a common practice for many research groups from all over the world, including Australia [11], Canada [12], France [13], Germany [14], Greece [15,16], Japan [17], United Arab Emirates [18,19], and USA [20–22].

Wastewater surveillance for SARS-CoV-2 can serve as an expansion of the clinical detection of infected individuals; this is owing to the fact that there is a possibility of underestimation of the disease's spread in the community, because of mild or asymptomatic carriers, if the detection is based only on clinical tests [18]. Furthermore, wastewater surveillance can be a useful tool in the case of low availability of clinical tests, and it also can serve as an early warning tool for the spread of COVID-19 in a community. A quantity of viral RNA detected in wastewater appears to have a correlation with clinical detected COVID-19 cases in corresponding sewersheds [19,20]. Moreover, in many cases, the detection of viral RNA in wastewater is possible days before first cases are reported by local authorities [23,24], and it

can foresee an upsurge in infections or hospitalizations [12,13,16,19,20,25,26]. Identification of the prevalence of a certain variant of the disease is also possible [27,28].

The presence of SARS-CoV-2 RNA in the feces, urine, or other excretions of COVID-19 patients has been recorded in various studies. A significant percentage of patients have shown positive fecal samples, while the presence of viral RNA in feces does not appear to be associated with the presence of gastrointestinal symptoms or with severity of illness; further, it seems that fecal samples remain positive longer than respiratory samples [29,30]. Less is known about exact shedding quantities, shedding duration, or correlation with the symptomatic phase.

Understanding the fate of SARS-CoV-2 RNA during its flow inside sewerage pipelines is crucial for properly assessing SARS-CoV-2 RNA quantities in wastewater and the health status of the corresponding population; however, very little is known about its mechanisms.

In a sewerage system, several microbial, chemical, and physicochemical processes take place, which affect viruses' fate during transport [31]. Coronaviruses are enveloped viruses that have a lipid bilayer membrane outside the viral protein capsid, which contains proteins or glycoproteins [32]. This kind of structure may have an impact on the viruses' survival in aqueous environments, where their lipid layers are sensitive to detergents and organic solvents [32]. Coronavirus is found to die off very rapidly in wastewater; thus, while genetic fragments remain detectable in wastewater, the virus most likely becomes nonviable once the envelope is damaged [32–34]. The survival of coronavirus in water depends on a number of factors, including temperature, light exposure (solar or UV inactivation), organic matter, total dissolved solids (TDS), hardness, turbidity, pH, nitrate concentrations, and the presence of antagonist microorganisms [35].

A few studies have paid closer attention to processes in sewerage systems. Petala et al. [15] examine the effect of environmental parameters on the adsorption of a virus onto suspended solids and found the ratio of the specific absorption (UV254/DOC) over the dissolved oxygen (DO) to be the parameter with the highest correlation with the viral copies. Kostoglou et al. [36] developed a general model for the absorption of SARS-CoV-2 parts on solid particles suspended in wastewater into a sewer system. Hart et al. [37] estimated the decay rate of several biomarkers into sewer systems, based on wastewater temperature, and examined the effect of seasonality and travel time on the SARS-CoV-2 loads available for observation at downstream monitoring locations [38].

The available studies inspect SARS-CoV-2 RNA's persistence in wastewater under storage conditions in the laboratory. The measured mean first-order decay rate constant (k) of SARS-CoV-2 ranges from 0.08–3.4 day^{-1} and T_{90} (time required for 90% reduction) between 3.3–52 days, for untreated wastewater, considering temperatures in the range of 4–37 °C. The tested material is either seeded raw wastewater samples [39–41] or positive raw wastewater samples [14,42]. All of the reviewed studies assume first-order decay of SARS-CoV-2 RNA. Bivins et al. [40] also examined the biphasic decay model for infectious SARS-CoV-2 using the sum-of-squares F test; they found that this did not improve the fit of the model, so they used only the first-order decay model for further analysis. Hokajarvi et al. [41] tested the log-linear and biphasic decay models and concluded to a linear decay of SARS-CoV-2 RNA at 4 °C.

Taking samples from the influent of WWTPs has been the main practice used for wastewater surveillance of COVID-19 spread to date, mainly because of convenience. This method has been proven to offer adequate information on the disease's spread in the corresponding sewershed. However, some weaknesses were not foreseen, such as the possibility of loss of information because of dilution, decay, or other processes inside sewerage pipelines, and the absence of more detailed monitoring of the spatial distribution of virus spread in the sewershed. Sampling at more points upstream in the sewer system, such as pumping stations, interceptors and manholes, has to be considered. In order to find the most appropriate sampling points, an optimization methodology is applied herein using an optimization algorithm.

Genetic algorithms are a very popular and strong optimization tool. A collection of several applications of genetic algorithms on water resources management can be found in [43]. Optimization algorithms can be useful in the selection of monitoring points for water quality observations; however, determining the objective function is the first and most important step. During the Battle of the Water Sensor Networks (BWSN), a group of design objectives for optimal sensor network design concerning water distribution systems was suggested [44]. These included time of detection, population affected, consumption of contaminated water, and detection likelihood. These objectives been used by several researchers to establish a network of monitoring points, able to detect contamination events in water distribution systems [45–47]. Banik et al. [48,49] used detection time and possibility of detection as design objectives for the optimal design of a sensor network for monitoring water quality parameters in a sewerage system. Also, Banik et al. [50] proposed joint entropy as a measure of information content and total correlation as objective functions, based on information theory. Lee et al. [51] proposed a methodology based on entropy theory for optimal water quality monitoring points in sewer systems, and Alfonso et al. [52] used information theory for optimal placement of flow measurement points in a river. Brentan et al. [46] applied entropy theory, as a step following optimization procedure, to rank a pareto front of nondominated solutions and find the best one. Psarrou et al. [53] applied a genetic algorithm for choosing optimal locations for sewer mining implementation, based on the minimization of hydrogen sulfide production into sewerage and the maximization of water needs satisfaction.

In the field of wastewater-based epidemiology, Domokos et al. [54] proposed a methodology for the optimal placement of sampling points for the detection of SARS-CoV-2, based on calculated discharges at each point, aiming for each point to be representative of a specific segment of the network and the whole network to be observed. However, they contemplate not a hydraulic model but a GIS model.

In the present study, we make the first attempt to model the movement of SARS-CoV-2 RNA into a sewerage system. Parameters such as discharge points, initial concentration, and decay rate of viral RNA can affect the concentration and load values that appear in different points across the system. Sensitivity analysis is performed to assess the effect of different values of initial concentration and decay rate to the maximum concentration and detection time appearing in downstream nodes. Additionally, this study aims at proposing a methodology for optimal selection of the quantity and the combination of sampling points through a sewerage system with a view to assessing COVID-19 spread in the population. This can be achieved by examining the effect of parameters such as detection time, detection likelihood, and population served by each node of the system. Results from the hydraulic model are then inserted into the optimization algorithm NSGA-II in order to find the adequate number and combination of sampling points.

2. Materials and Methods

The proposed methodology includes a fate and transport modelling approach of SARS-CoV-2 RNA into urban sewer systems, followed by an optimization procedure for selecting optimal sampling points for COVID-19 spread surveillance. Time series data of SARS-CoV-2 RNA concentration across the sewer system are obtained under different scenarios, executed using the SWMM model. These data are used as input for running the NSGA-II optimization algorithm and selecting optimal sampling points and an adequate number of sampling locations. Finally, decision-making methods are applied as a supportive tool.

A brief description of the methodology used in this study is presented in the flowchart illustrated in Figure 1.

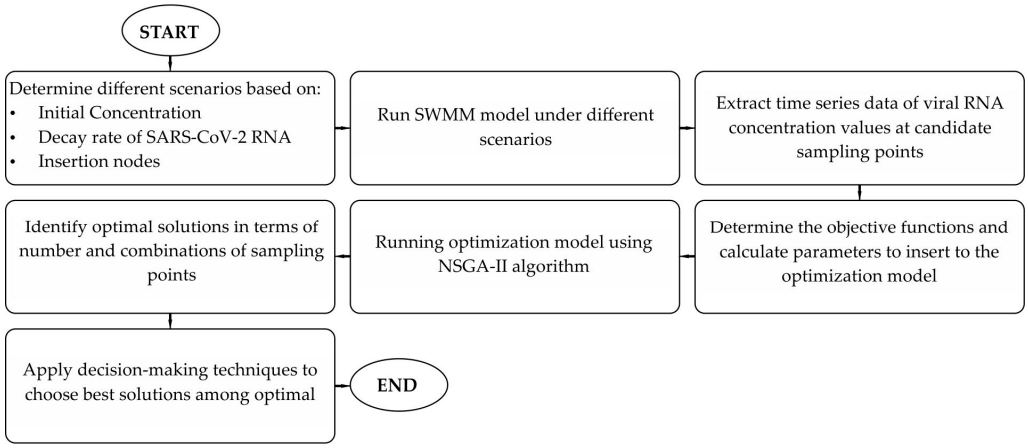

Figure 1. Workflow of the optimization methodology.

2.1. SWMM

The United States Environmental Protection Agency's Storm Water Management Model (EPA's SWMM) is used for the simulation of SARS-CoV-2 RNA fate and transport in sewer systems. SWMM is a dynamic rainfall runoff simulation model; it also contains a flexible set of hydraulic modelling capabilities used to rout runoff, external inflows, and water quality constituents through the drainage system [55]. It is possible for the user to enter dry weather sanitary flows and user-specified external inflows at any point in the drainage system. As a result, SWMM can be used to simulate combined sewer systems as well as to separate drainage and sewer systems [56]. For water quality constituent routing, SWMM computations are based on one-dimensional advection—dispersion equation (Equation (1)) for the transport of dissolved constituents along the length of a conduit [57]:

$$\frac{\partial c}{\partial t} = -\frac{\partial (uc)}{\partial x} + \frac{\partial}{\partial x}\left(D\frac{\partial c}{\partial x}\right) + r(c) \quad (1)$$

where c: constituent concentration (ML^{-3}), u: longitudinal velocity (LT^{-1}), D: longitudinal dispersion coefficient (L^2/T), $r(c)$: reaction rate term ($ML^{-3}T^{-1}$)), x: longitudinal distance (L), and t: time (T). SWMM assumes conduits to operate as completely mixed reactors and uses (Equation (2)) to solve constituents' transport into the sewer system [57]:

$$\frac{\partial (Vc)}{\partial t} = C_{in}Q_{in} - cQ_{out} - Vr(c) \quad (2)$$

where V: volume within the reactor, c: concentration within the reactor, C_{in}: concentration of any inflow to the reactor, Q_{in}: volumetric flow rate of this inflow, Q_{out}: volumetric flow rate leaving the reactor, and $r(c)$: a function that determines the rate of loss due to reaction. To account for the reaction term, a constant first-order decay rate is assumed for the present study.

It is assumed that SARS-CoV-2 RNA decay in wastewater follows the first-order decay (Equation (3)) as long as there are no more specific data available to run a more sophisticated model; first-order decay has been also suggested in other studies [22,37,39,40,58], as previously mentioned.

$$C = C_0 e^{-kt} \quad (3)$$

where C: SARS-CoV-2 concentration, k: first-order decay rate constant.

Simulation results for SARS-CoV-2 RNA concentration at each node of the system are extracted from the SWMM model using the pyswmm Python library [59].

2.2. Optimization

For performing the optimization procedure, a number of scenarios were considered. The relatively low value of 3×10^4 gene copies/L (GC/L) was chosen for the initial concentration of virus discharging into the sewer system, from one insertion point at a time; for the decay rate, the relatively high value equal to 3.36 day^{-1} was considered. In order to reduce computational time, sixteen different insertion points of the virus across the sewer system were examined (Figure 2a), and nodes with the higher values of base flow were chosen. Furthermore, 21 nodes were evaluated as possible sampling points (Figure 2b) based on their placement into the sewer system. Nodes located at central areas of the city and nodes where multiple branches contribute were chosen. The outfall node to the WWTP was also included. The time series of concentration at all candidate nodes was extracted from the SWMM simulation results, then they were used to calculate parameters required as an input to the optimization model. The average values of detection time (T_d) and detection likelihood (D_L) were calculated for each control node, under all scenarios. Additionally, the population served (P_s) from each control node was estimated. These values were then imported into the optimization model.

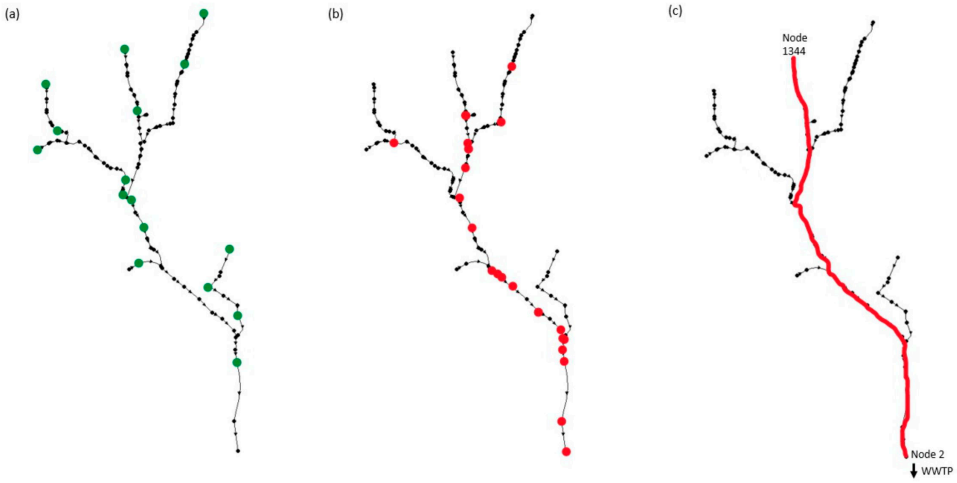

Figure 2. Sewerage system of the city of Kozani with denoted: (**a**) simulated insertion points, (**b**) simulated candidate sampling points, (**c**) sewerage path from insert node 1344 to candidate sampling node 2 (outfall to the WWTP); across this path, indicative results of simulation are presented.

The optimal selection of sampling points combinations aims to be able to detect quickly the SARS-CoV-2 traces reliable, and to be representative of as many individuals as possible. This concept can be realized through a multi-objective optimization problem. Detection time was proposed by [44] as an objective function for optimal sensor location for hazardous pollutant detection in water distribution systems, which is also used by [49] for sewer systems' water quality monitoring. Ostfeld et al. [44] also proposed detection likelihood and affected population as objective functions. Hereafter, the three objective functions that are evaluated in this study are described:

Detection time (T_d). T_d is the elapsed time from the start of viral shedding to the sewer system until the first detection at the node. Its values are generated from the SWMM model results, considering a limit of detection (LOD) equal to 10^3 GC/L. In the case that the concentration at a node never reaches the LOD during the whole simulation time, it is not taken into account. Average detection time (T_d) for a certain combination is used for the optimization.

$$T_d = \frac{\sum_1^N T_d(X_i)}{N}, \qquad i = 1 \ldots N \tag{4}$$

where T_d (X_i) is the first detection time at the sampling point (node) X_i, and N is the number of selected sampling points.

Population (P_s) is the upstream population (P_s) that is connected to a particular node. In maximum population (P_s), that which can be represented from a certain combination is considered.

$$P_s = \max P_s\ (X_i), \qquad i = 1 \ldots . N \tag{5}$$

where $P_s\ (X_i)$ is the upstream population connected to a sampling point (node) *Xi.*

Detection likelihood (D_L), at each node. Average detection likelihood (D_L) for a certain combination is used for the optimization:

$$D_L = \frac{\sum_i^N D_L(X_i)}{N}, \qquad i = 1 \ldots . N \tag{6}$$

where $D_L\ (X_i)$ is the detection likelihood at a particular node *Xi*, D_L is equal to 1 if the viral RNA is detected and equal to 0 otherwise.

Thus, the multi-objective optimization problem was performed with three different combinations of objective functions as described in the following Equations (7)–(9):

$$\text{Combination 1: } f_1 = \min T_d,\ f_2 = \max D_L \tag{7}$$

$$\text{Combination 2: } f_1 = \min T_d,\ f_2 = \max P_s \tag{8}$$

$$\text{Combination 3: } f_1 = \min T_d,\ f_2 = \max Ps,\ f_3 = \max D_L \tag{9}$$

The optimization problem was solved by the nondominated sorting genetic algorithm (NSGA-II), a multi-objective evolutionary algorithm proposed by [60]. The NSGA-II algorithm achieves alleviation of computational complexity by introducing a fast nondominated sorting procedure and a selection operator that creates a mating pool by combining the parent and offspring populations and selecting the best solutions in terms of fitness and spread. The main operations of the algorithm are nondominated sorting, crowding-distance calculation, and sorting based on a crowding-comparison operator [60]. For realization of the optimization methodology, the pymoo Python library was used [61].

2.3. Study Area

The proposed methodology was applied to the sewer system of the city of Kozani located in Western Macedonia, Greece, as shown in Figure 3. The region of Kozani was one of the areas of Greece most affected by the COVID-19 pandemic, with 48.5% of the population diagnosed with COVID-19 between 2020 and 2022 [62]. The city of Kozani has a combined sewerage system that collects wastewater and stormwater and conveys them to the local treatment plant; there is also a combined sewer overflow outfall in front of the entrance to the treatment plant in the event of intense rainfall. The local wastewater treatment plant (WWTP) serves about 49,000 inhabitants from the city of Kozani and the nearby suburban area of Krokos. The WWTP receives mainly residential wastewater, and there is a hospital in the area. Data about the geometry of the sewer system were obtained from the local water supply and sewerage services company. The available data included nodes' coordinates, maximum depth, and incomplete elevation data, along with conduits' length, cross-section geometry, and material. Due to the lack of complete data, only the main branches of the sewerage system were used in the present analysis. The wastewater inflows at each node of the system were unknown, thus they were estimated based on the service area of each node, statistical data on population density, and the data of the inflow to the WWTP. For the data preparation and estimation of each node service area, QGIS software, version 3.16.11 was used, and at nodes where the elevation is not known, it was extracted from the digital elevation model (DEM) acquired from Copernicus, Land Monitoring Service. The system was studied under dry weather conditions. Constant flow of domestic wastewater was assumed, and no hourly patterns were taken into consideration.

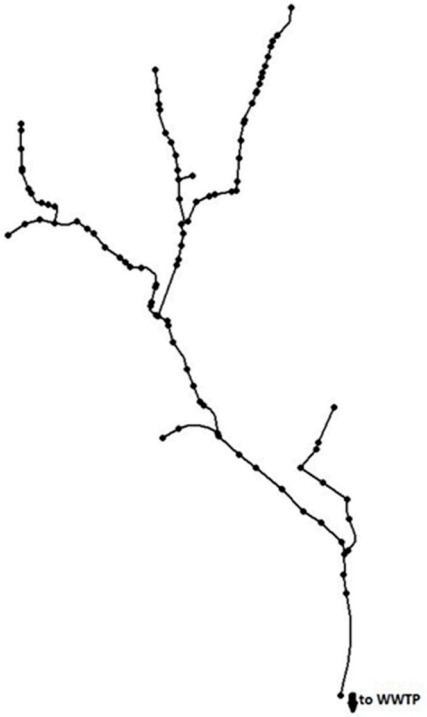

Figure 3. Sewerage system of the city of Kozani, Western Macedonia, Greece.

Several scenarios were examined under dry weather conditions considering different values of the initial concentration of SARS-CoV-2, the decay rate of viral RNA, and all the possible insertion points across the sewer system. Continuous discharge of SARS-CoV-2 was assumed, during the 24 h simulation time, with initial concentration between 3×10^4 gene copies/L (GC/L) and 15×10^4 GC/L. Since the reported concentration values in wastewater from the available studies are of different orders of magnitude and no standardized discharge concentration values per person exist, the values used here were derived as multipliers of the limit of detection (LOD). The LOD of SARS-CoV-2 in wastewater was assumed to be in the range of 1,000–3,000 GC/L [16,22,63].

In this study, a first-order decay rate constant in the range of 0.1 to 3.4 day^{-1} [22,39,40] was considered, assuming average wastewater temperatures in the range of 15–25 °C [37,38,64]. Wastewater temperature appears to have a positive correlation with the decay of SARS-CoV-2 RNA; the higher the temperature, the higher the decay rate [65].

3. Results and Discussion

3.1. Simulation Results and Sensitivity Analysis

Different scenarios were simulated using SWMM model; four values of decay rate and initial concentration were considered, and various SARS-CoV-2 insertion points were evaluated. The results of the simulations and optimization are presented in the rest of this manuscript.

The indicative SWMM simulation results are reported in Figures 4 and 5a,b. Results for candidate sampling nodes located on the sewerage path between node 1344 (the virus's entrance point) and node 2 (the outfall to WWTP) (Figure 2c) are included. Figure 4 presents the maximum total inflow (L/s) at each node. Figure 5a presents the peak concentration (C_{max}) and detection time (T_d) at each node under four different values of decay rate, in the range of values referred to in the reviewed bibliography. Meanwhile, Figure 5b shows the peak concentration and detection time at each node under four different values of initial concentration. The nodes appear from left to right, from upstream to downstream. The maximum total inflow increases from upstream to downstream, and a sharper rise appears after an extra branch contributes its flow to the main path. At the same nodes, an acute reduction of peak concentration also appears for the combination of all simulation

parameters, due to dilution. Likewise, peak concentration is reduced while travel time increases, because of the effect of decay. Downstream nodes where the entrance to the treatment plant is located show a notable decline in the peak concentration. The effect of the decay rate and the dilution is significant; considering that few data are available for fate and transport of the SARS-CoV-2 RNA value, this leads to a great deal of uncertainty in the analysis of SARS-CoV-2 RNA presence in samples coming from the entrance to the WWTP, which is the common practice during wastewater surveillance. As expected, the detection time of SARS-CoV-2 RNA at each node is increased with the distance from the discharge point.

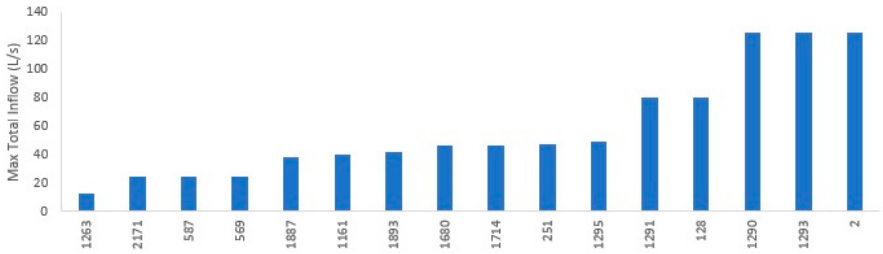

Figure 4. Simulation results for maximum total inflow (L/s), across candidate sampling nodes located on the sewerage path between node 1344 and node 2.

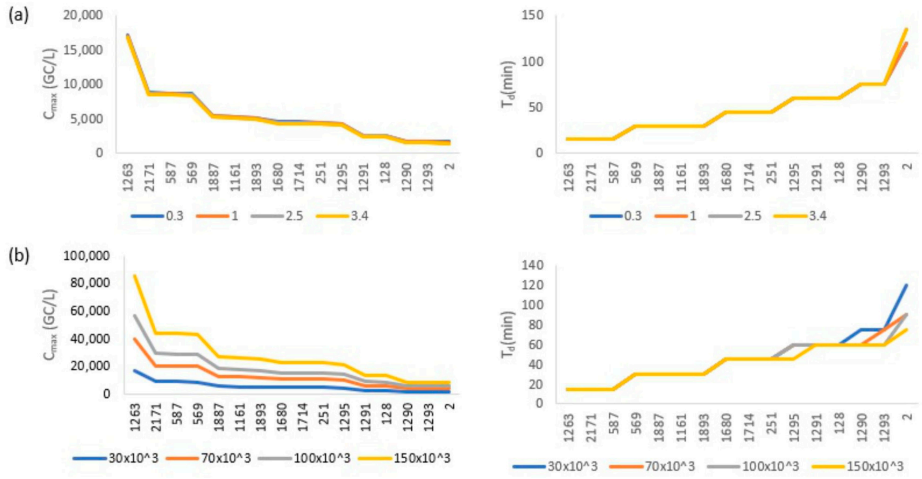

Figure 5. Sensitivity analysis results and simulation results for: (**a**) C_{max} and (**b**) T_d.

In the present study, maximum concentration values at node 2 (entrance to WWTP) are found between 1,377–7,979 GC/L. The available data from other studies report concentration values of the WWTPs' influent in the range of 100–100,000 GC/L (capacity 57,000–200,000 m^3/day) [20], 750–34,000 GC/L (capacity 5,200–241,000 m^3/day) [18], 12–22,000 GC/L [23], and 3,000–20,000 GC/L (capacity 13,400–1,100,000 m^3/day) [14]. Direct comparisons are not possible because of the different capacities of the studied WWTPs and the unknown or roughly estimated number of infected persons. However, our simulated data are in the reported range of these studies, in the low side of them, which is expected since the WWTP under study have a lower capacity (16,500 m^3/day) than the WWTPs studied elsewhere. Furthermore, in the present study, the viral load insertion is assumed to be only in one node at a time, in order to simulate the case of a low number of infected persons and an early detection of the disease surge. The concentration data along the sewer system are spears; however, the reported values of 286–29,000 GC/L [18] are of the same order of magnitude as the simulated values of the present study.

Sensitivity analysis was performed for examining how different values of the input parameters affect the model's outputs. In the present study, the decay rate and initial concentration of SARS-CoV-2 are tested for their effect on maximum concentration and detection time (Figure 5). It is evident that decay rate values have no significant effect on

either maximum concentration or detection time. The maximum concentration values are slightly different, and the detection time values are almost the same except for the three last nodes, especially node 2 (in front of the entrance to the WWTP). However, the patterns are similar across the sewer system and, as a result, the optimization results are not expected to be affected. On the other hand, the different initial concentration values cause an important change in the maximum concentration values, especially in the nodes closer to the entrance point. Moreover, influence on detection time is less important and appears at the nodes with longer distance from the entrance point. More data will subsequently be needed on the virus's shedding quantities from infected persons for a better interpretation of the WBE data, although the optimization results may not be affected since the patterns are similar.

3.2. Optimization Results

Even though the best option for wastewater-based evaluation of SARS-CoV-2 prevalence in a sewershed is to take samples from all possible nodes, this may not be practical because of budget, time, personnel, or other constraints, and in this case only a certain number of sampling points have to be included. In this study, 21 nodes of the main path of the sewer pipeline network were evaluated as possible sampling points (Figure 2b), and sixteen nodes were considered as possible insertion points (Figure 2a). As long as sensitivity analysis results reveal a slight effect of tested input parameters, optimization methodology is applied under simulation results for 3×10^4 GC/L initial concentration and a decay rate equal to 3.4 day^{-1}. Using the NSGA-II optimization algorithm and assuming that a set of 1 to 10 sampling points (Ns) can be selected each time, the following results are derived. Figures 6 and 7 present optimization results for objective functions combination (1), (2) and (3), respectively. Each point represents a solution and the values of objective function that can be achieved with each one of them. For the sewer system under study, four to six sampling points appear to be adequate to acquire representative samples and to allow the detection of SARS-CoV-2 RNA quickly and reliably, under all combinations of objective functions. A set of two sampling points also performs well in some cases (e.g., combination 1), though in other cases it is not (e.g., combination 2). Thus, they are not proposed as a possible optimal solution, in this study. On the other hand, increasing the number of sampling points to more than six does not seem to further improve the value of the objective functions under all the examined combinations. Domokos et al. [54] also concluded to the selection of six sampling points as an optimal placement of measurement points for SARS-CoV-2 measurements into the sewer system of a small city in Hungary.

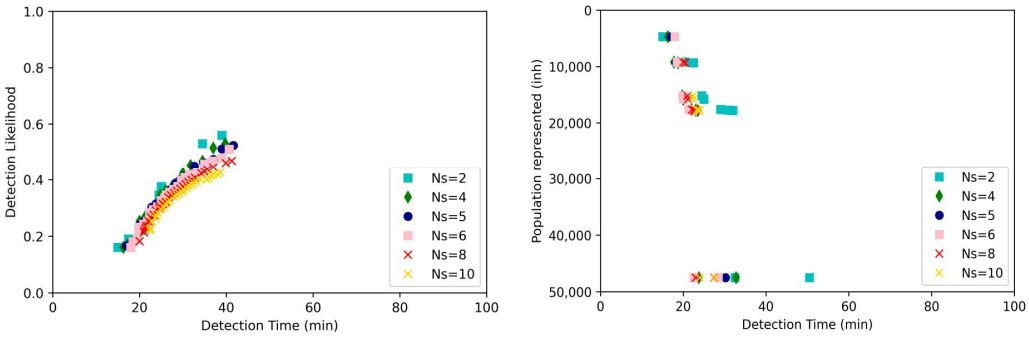

Figure 6. Optimization's results under combination (1) of objective functions: detection time (T_d) and detection likelihood (D_L) and combination (2) of objective functions: population represented (P_s) and detection time (T_d).

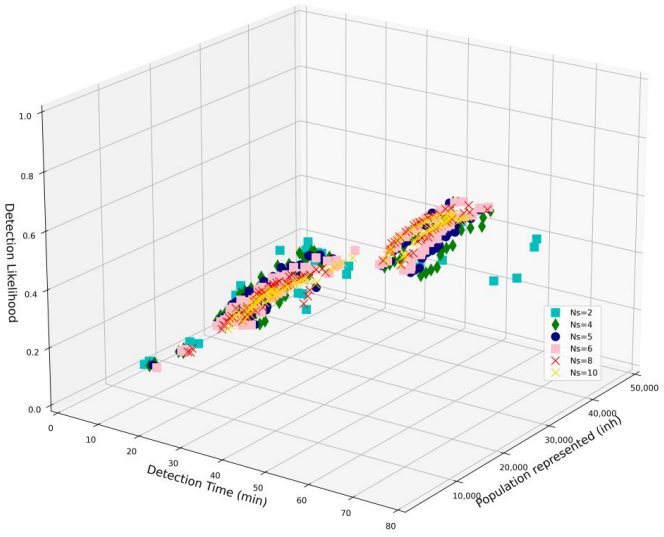

Figure 7. Optimization's results under combination (3) of objective functions: population represented (P_s), detection time (T_d) and detection likelihood (D_L).

3.3. Decision Making

Due to large number of optimal solutions derived from the multi-objective optimization procedure, a decision-making step is necessary. This step may be applied by decision makers, based on their critical thinking, or a decision-making technique can be engaged. By means of mathematics, all solutions are equal. Since objective functions are conflicting, choosing a solution that improves one parameter, this comes at the cost of deteriorating another one. A two-step procedure with multi-objective optimization as a first step, followed by a decision-making technique as a second step, is implemented in the present study. In order to reduce the search area, the decision-making technique is applied only for optimal solutions derived from combinations of 4, 5, and 6 sampling points, which are found to give the best results among all the tested combinations. The Technique for order of preference by similarity to ideal solution (TOPSIS) [66] is utilized herein as the decision-making step. With the TOPSIS method, optimal solutions are sorted based on how close they are to the positive ideal solution and how far they are from the negative ideal solution. Although simple, it is found to be among the best methods by [67], who made a comparative study of well-established methods for selection amid nondominated optimal solutions, formulated by multi-objective optimization procedure. The TOPSIS results for the first four ranked solutions are presented in Table 1 for each optimization combination. Also, the Simple Additive Weighting (SAW) method [68] and ranking based on detection likelihood were tested in the present study, and the results for combination C3 are presented in Table 1. Both the TOPSIS and the SAW methods are proposed as solutions that are representative for the whole population. The first four selected solutions by the TOPSIS method yield a detection likelihood of more than 0.3 ($D_L > 0.30$) and a detection time of less than 48 min ($T_d < 48$ min), while those selected by the SAW method yield $D_L > 0.46$ and $T_d < 42$ min. On the other hand, sorting solutions based on D_L values suggests higher values of detection likelihood ($D_L > 0.50$) and similar levels of detection time ($T_d < 43$ min). However, the represented population is lower (no more than 18,500 inhabitants). In general, the SAW method appears to have slightly better performance than TOPSIS, in terms of the proposed solutions, and both methods seem to have better performance than a sorting solution based on detection likelihood.

Table 1. Decision-making results of optimal solutions that ranked in the four first places for each optimization combination (C1, C2 and C3) (Ns: number of sampling points, T_d: detection time, P_s: population represented, D_L: detection likelihood).

Optimization Combination	Ns	Solutions	T_d (min)	P_S (inh)	D_L
WWTP	1		86	47,494	0.25
TOPSIS					
C1	4	1872, 1161, 1893, 1295	39.75		0.53
	4	1872, 1161, 251, 1295	37		0.52
	4	1872, 1161, 1295, 1290	34.5		0.47
	4	1937, 1872, 1161, 1295	34.5		0.47
C2	6	1263, 1680, 1714, 1291, 128, 2	28.5	47,496	
	6	1263, 2171, 1680, 1714, 1291, 128	22.5	47,494	
	4	1263, 1680, 128, 2	32.75	47,496	
	4	1263, 2171, 1680, 128	23.75	47,494	
C3	4	1161, 1680, 1295, 2	44.75	47,496	0.39
	4	1872, 251, 1295, 2	47.75	47,496	0.44
	4	1937, 2171, 1680, 1295	31.5	47,494	0.31
	4	1680, 1295, 1291, 2	39	47,496	0.30
SAW					
C3	4	1872, 2171, 1161, 1295	40.5	47,494	0.47
	5	1872, 2171, 1161, 1893, 1295	41.8	47,494	0.47
	5	1872, 2171, 1161, 251, 1295	39.6	47,494	0.46
	6	1872, 2171, 1161, 1893, 251, 1295	40.8	47,494	0.47
Sorted based on D_L					
C3	4	1872, 1161, 1893, 1295	39.75	17,731	0.53
	4	2185, 1872, 1161, 1295	40.25	17,814	0.53
	5	2185, 1872, 1161, 1893, 1295	41.6	17,814	0.52
	4	1872, 1887, 1161, 1295	43	18,532	0.52

Sampling only from the WWTP influent, which is the common practice, appears to have a worse performance, obtaining D_L = 0.25, T_d = 86 min. Samples of the WWTP's entrance can be representative of the whole population, though sampling at various points across the sewer system can offer insight about the space distribution of disease prevalence. Furthermore, sampling near the source diminishes the decay and dilution effect, and it can be an effective tool for accurate estimation of the number of infected persons [69].

Furthermore, Figure 8 depicts the 1st ranked solutions derived from the TOPSIS and SAW methods and sorting based on detection likelihood under C3 optimization combination. It is apparent that the solutions are well allocated throughout the sewer system. Spread measurement points across the sewer system are proposed by Banik et al. [48] for water quality monitoring and by Domokos et al. [54] for SARS-CoV-2 monitoring; both of these methods include WWTP as part of the optimal solution. Moreover, the solutions are overlapping at certain nodes.

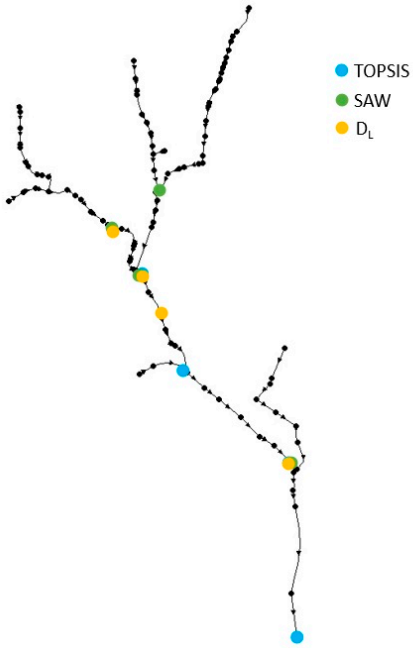

Figure 8. 1st ranked solution derived from TOPSIS and SAW methods and sorting based on D_L under C3 optimization combination.

4. Conclusions

In this study, simulation of the fate and transport of SARS-CoV-2 RNA and a methodology to determine the optimal sampling points in terms of number and combinations for wastewater surveillance were applied. The sewerage system of the city of Kozani was used for testing the proposed methodology. The proposed methodology can be useful for wastewater-based monitoring of future virus strikes and pandemics. SWMM was used for the modelling procedure, followed by the application of the NSGA-II optimization algorithm and a decision-making procedure in order to choose the appropriate sampling points. Several scenarios were considered, and the results show that parameters such as the initial concentration and decay rate of SARS-CoV-2 have an impact on concentration and detection time at downstream nodes. This impact is more obvious when the distance from the insertion point is bigger. The optimization results indicate that for the network under study, combinations of 4 to 6 sampling points are sufficiently informative for SARS-CoV-2 RNA presence. They are representative of all the population and allow a reliable detection of viral RNA, with more than 30% likelihood. Additionally, very soon after the first release into the sewer system, a detection of SARS-CoV-2 with an average time of 40 min is possible. Yet if a bigger part of the sewer system is modelled, the travel time and consequently the detection time will be longer. Sampling more than six points does not appear to further improve the detection time or detection likelihood. Decision-making techniques are used as a supportive tool due to the large number of optimal results. Solutions that are ranked first have some nodes in common and are well spread along the sewer system. Additionally, selecting sampling points located at different locations across the sewer system seems to be more informative than sampling at a single downstream location. Comparing the results of the present study with the case of taking samples for the WWTP's entrance, it is revealed that a higher detection likelihood and a lower detection time can be yielded if the measurement points are more scattered across the sewerage. It must be mentioned that since the shedding concentration per infected person and the decay rate in wastewater are barely known, it is apparent that there is great uncertainty in any attempt to simulate the fate and transport of viral particles and fragments into the sewer system. More research is needed to determine parameters such as shedding duration, shedding rate per person, and persistence of viral RNA in wastewater.

Author Contributions: Conceptualization, A.G. and A.Z.; methodology, A.G.; software, A.G.; validation, A.G.; formal analysis, A.G.; investigation, A.G.; resources, A.G. and A.Z.; data curation, A.G.; writing—original draft preparation, A.G.; writing—review and editing, A.G. and A.Z.; visualization, A.G.; supervision, A.Z.; project administration, A.G. and A.Z. All authors have read and agreed to the published version of the manuscript.

Funding: This research received no external funding.

Data Availability Statement: Data are contained within the article.

Acknowledgments: The authors would like to thank I. Gkanatsa and I. Goudios from the municipality of Kozani Water Supply and Sewerage services Company for providing the sewerage system data.

Conflicts of Interest: The authors declare no conflict of interest.

References

1. Ibáñez, M.; Borova, V.; Boix, C.; Aalizadeh, R.; Bade, R.; Thomaidis, N.S.; Hernández, F. UHPLC-QTOF MS Screening of Pharmaceuticals and Their Metabolites in Treated Wastewater Samples from Athens. *J. Hazard. Mater.* **2017**, *323*, 26–35. [CrossRef]
2. Galani, A.; Alygizakis, N.; Aalizadeh, R.; Kastritis, E.; Dimopoulos, M.; Thomaidis, N.S. Environment Patterns of Pharmaceuticals Use during the Fi Rst Wave of COVID-19 Pandemic in Athens, Greece as Revealed by Wastewater-Based Epidemiology. *Sci. Total Environ.* **2021**, *798*, 149014. [CrossRef] [PubMed]
3. Birošová, L.; Mackuľak, T.; Bodík, I.; Ryba, J.; Škubák, J.; Grabic, R. Pilot Study of Seasonal Occurrence and Distribution of Antibiotics and Drug Resistant Bacteria in Wastewater Treatment Plants in Slovakia. *Sci. Total Environ.* **2014**, *490*, 440–444. [CrossRef] [PubMed]
4. Han, J.; He, S. Urban Flooding Events Pose Risks of Virus Spread during the Novel Coronavirus (COVID-19) Pandemic. *Sci. Total Environ.* **2021**, *755*, 142491. [CrossRef] [PubMed]
5. Rousis, N.I.; Denardou, M.; Alygizakis, N.; Galani, A.; Bletsou, A.A.; Damalas, D.E.; Maragou, N.C.; Thomas, K.V.; Thomaidis, N.S. Assessment of Environmental Pollution and Human Exposure to Pesticides by Wastewater Analysis in a Seven-Year Study in Athens, Greece. *Toxics* **2021**, *9*, 260. [CrossRef] [PubMed]
6. Lodder, W.J.; Buisman, A.M.; Rutjes, S.A.; Heijne, J.C.; Teunis, P.F.; de Roda Husman, A.M. Feasibility of Quantitative Environmental Surveillance in Poliovirus Eradication Strategies. *Appl. Environ. Microbiol.* **2012**, *78*, 3800–3805. [CrossRef] [PubMed]
7. Ivanova, O.E.; Yarmolskaya, M.S.; Eremeeva, T.P.; Babkina, G.M.; Baykova, O.Y.; Akhmadishina, L.V.; Krasota, A.Y.; Kozlovskaya, L.I.; Lukashev, A.N. Environmental Surveillance for Poliovirus and Other Enteroviruses: Long-Term Experience in Moscow, Russian Federation, 2004–2017. *Viruses* **2019**, *11*, 424. [CrossRef]
8. Suffredini, E.; Iaconelli, M.; Equestre, M.; Valdazo-González, B.; Ciccaglione, A.R.; Marcantonio, C.; Della Libera, S.; Bignami, F.; La Rosa, G. Genetic Diversity Among Genogroup II Noroviruses and Progressive Emergence of GII.17 in Wastewaters in Italy (2011–2016) Revealed by Next-Generation and Sanger Sequencing. *Food Environ. Virol.* **2018**, *10*, 141–150. [CrossRef]
9. Hou, C.; Hua, Z.; Xu, P.; Xu, H.; Wang, Y.; Liao, J.; Di, B. Estimating the Prevalence of Hepatitis B by Wastewater-Based Epidemiology in 19 Cities in China. *Sci. Total Environ.* **2020**, *740*, 139696. [CrossRef]
10. Wang, X.W.; Li, J.; Guo, T.; Zhen, B.; Kong, Q.; Yi, B.; Li, Z.; Song, N.; Jin, M.; Xiao, W.; et al. Concentration and Detection of SARS Coronavirus in Sewage from Xiao Tang Shan Hospital and the 309th Hospital of the Chinese People's Liberation Army. *Water Sci. Technol.* **2005**, *52*, 213–221. [CrossRef]
11. Ahmed, W.; Angel, N.; Edson, J.; Bibby, K.; Bivins, A.; O'Brien, J.W.; Choi, P.M.; Kitajima, M.; Simpson, S.L.; Li, J.; et al. First Confirmed Detection of SARS-CoV-2 in Untreated Wastewater in Australia: A Proof of Concept for the Wastewater Surveillance of COVID-19 in the Community. *Sci. Total Environ.* **2020**, *728*, 138764. [CrossRef] [PubMed]
12. D'Aoust, P.M.; Graber, T.E.; Mercier, E.; Montpetit, D.; Alexandrov, I.; Neault, N.; Baig, A.T.; Mayne, J.; Zhang, X.; Alain, T.; et al. Catching a Resurgence: Increase in SARS-CoV-2 Viral RNA Identified in Wastewater 48 h before COVID-19 Clinical Tests and 96 h before Hospitalizations. *Sci. Total Environ.* **2021**, *770*, 145319. [CrossRef] [PubMed]
13. Wurtzer, S.; Marechal, V.; Mouchel, J.M.; Maday, Y.; Teyssou, R.; Richard, E.; Almayrac, J.L.; Moulin, L. Evaluation of Lockdown Effect on SARS-CoV-2 Dynamics through Viral Genome Quantification in Waste Water, Greater Paris, France, 5 March to 23 April 2020. *Eurosurveillance* **2020**, *25*, 2000776. [CrossRef] [PubMed]
14. Westhaus, S.; Weber, F.A.; Schiwy, S.; Linnemann, V.; Brinkmann, M.; Widera, M.; Greve, C.; Janke, A.; Hollert, H.; Wintgens, T.; et al. Detection of SARS-CoV-2 in Raw and Treated Wastewater in Germany—Suitability for COVID-19 Surveillance and Potential Transmission Risks. *Sci. Total Environ.* **2021**, *751*, 141750. [CrossRef] [PubMed]
15. Petala, M.; Dafou, D.; Kostoglou, M.; Karapantsios, T.; Kanata, E.; Chatziefstathiou, A.; Sakaveli, F.; Kotoulas, K.; Arsenakis, M.; Roilides, E.; et al. A Physicochemical Model for Rationalizing SARS-CoV-2 Concentration in Sewage. Case Study: The City of Thessaloniki in Greece. *Sci. Total Environ.* **2020**, *755*, 142855. [CrossRef] [PubMed]
16. Galani, A.; Aalizadeh, R.; Kostakis, M.; Markou, A.; Alygizakis, N.; Lytras, T.; Adamopoulos, P.G.; Peccia, J.; Thompson, D.C.; Kontou, A.; et al. SARS-CoV-2 Wastewater Surveillance Data Can Predict Hospitalizations and ICU Admissions. *Sci. Total Environ.* **2022**, *804*, 150151. [CrossRef] [PubMed]

17. Hata, A.; Hara-Yamamura, H.; Meuchi, Y.; Imai, S.; Honda, R. Detection of SARS-CoV-2 in Wastewater in Japan during a COVID-19 Outbreak. *Sci. Total Environ.* **2021**, *758*, 143578. [CrossRef] [PubMed]
18. Hasan, S.W.; Ibrahim, Y.; Daou, M.; Kannout, H.; Jan, N.; Lopes, A.; Alsafar, H.; Yousef, A.F. Detection and Quantification of SARS-CoV-2 RNA in Wastewater and Treated Effluents: Surveillance of COVID-19 Epidemic in the United Arab Emirates. *Sci. Total Environ.* **2021**, *764*, 142929. [CrossRef]
19. Albastaki, A.; Naji, M.; Lootah, R.; Almeheiri, R.; Almulla, H.; Almarri, I.; Alreyami, A.; Aden, A.; Alghafri, R. First Confirmed Detection of SARS-CoV-2 in Untreated Municipal and Aircraft Wastewater in Dubai, UAE: The Use of Wastewater Based Epidemiology as an Early Warning Tool to Monitor the Prevalence of COVID-19. *Sci. Total Environ.* **2021**, *760*, 143350. [CrossRef]
20. Gonzalez, R.; Curtis, K.; Bivins, A.; Bibby, K.; Weir, M.H.; Yetka, K.; Thompson, H.; Keeling, D.; Mitchell, J.; Gonzalez, D. COVID-19 Surveillance in Southeastern Virginia Using Wastewater-Based Epidemiology. *Water Res.* **2020**, *186*, 116296. [CrossRef]
21. Wu, F.; Xiao, A.; Zhang, J.; Moniz, K.; Endo, N.; Armas, F.; Bonneau, R.; Brown, M.A.; Bushman, M.; Chai, P.R.; et al. SARS-CoV-2 Titers in Wastewater Foreshadow Dynamics and Clinical Presentation of New COVID-19 Cases. *medRxiv* **2020**, 1–44. [CrossRef]
22. Weidhaas, J.; Aanderud, Z.T.; Roper, D.K.; VanDerslice, J.; Gaddis, E.B.; Ostermiller, J.; Hoffman, K.; Jamal, R.; Heck, P.; Zhang, Y.; et al. Correlation of SARS-CoV-2 RNA in Wastewater with COVID-19 Disease Burden in Sewersheds. *Sci. Total Environ.* **2021**, *775*, 145790. [CrossRef] [PubMed]
23. Medema, G.; Heijnen, L.; Elsinga, G.; Italiaander, R.; Brouwer, A. Presence of SARS-Coronavirus-2 RNA in Sewage and Correlation with Reported COVID-19 Prevalence in the Early Stage of the Epidemic in the Netherlands. *Environ. Sci. Technol. Lett.* **2020**, *7*, 511–516. [CrossRef] [PubMed]
24. Randazzo, W.; Truchado, P.; Cuevas-Ferrando, E.; Simón, P.; Allende, A.; Sánchez, G. SARS-CoV-2 RNA in Wastewater Anticipated COVID-19 Occurrence in a Low Prevalence Area. *Water Res.* **2020**, *181*, 115942. [CrossRef] [PubMed]
25. Nemudryi, A.; Nemudraia, A.; Wiegand, T.; Surya, K.; Buyukyoruk, M.; Cicha, C.; Vanderwood, K.K.; Wilkinson, R.; Wiedenheft, B. Temporal Detection and Phylogenetic Assessment of SARS-CoV-2 in Municipal Wastewater. *Cell Rep. Med.* **2020**, *1*, 100098. [CrossRef] [PubMed]
26. Petala, M.; Kostoglou, M.; Karapantsios, T.; Dovas, C.; Lytras, T.; Paraskevis, D.; Roilides, E.; Koutsolioutsou-Benaki, A.; Panagiotakopoulos, G.; Sypsa, V.; et al. Relating SARS-CoV-2 Shedding Rate in Wastewater to Daily Positive Tests Data: A Consistent Model Based Approach. *Sci. Total Environ.* **2021**, *807*, 150838. [CrossRef] [PubMed]
27. Chassalevris, T.; Chaintoutis, S.C.; Koureas, M.; Petala, M.; Moutou, E.; Beta, C.; Kyritsi, M.; Hadjichristodoulou, C.; Kostoglou, M.; Karapantsios, T.; et al. SARS-CoV-2 Wastewater Monitoring Using a Novel PCR-Based Method Rapidly Captured the Delta-to-Omicron BA.1 Transition Patterns in the Absence of Conventional Surveillance Evidence. *Sci. Total Environ.* **2022**, *844*, 156932. [CrossRef]
28. Tiacharoen, V.; Denpetkul, T.; Kosoltanapiwat, N.; Maneekan, P.; Thippornchai, N.; Saeoueng, A.; Jittmittraphap, A.; Sattabongkot, J.; Leaungwutiwong, P. Detection of SARS-CoV-2 and Variants in Hospital Wastewater in a Developing Country. *Water* **2022**, *14*, 3798. [CrossRef]
29. Wu, F.; Zhang, J.; Xiao, A.; Gu, X.; Lee, L.; Armas, F.; Kauffman, K.; Hanage, W.; Matus, M.; Ghaeli, N.; et al. SARS-CoV-2 Titers in Wastewater Are Higher than Expected from Clinically Confirmed Cases. *mSystems* **2020**, *5*, e00614-20. [CrossRef]
30. Chen, Y.; Chen, L.; Deng, Q.; Zhang, G.; Wu, K.; Ni, L.; Yang, Y.; Liu, B.; Wang, W.; Wei, C.; et al. The Presence of SARS-CoV-2 RNA in the Feces of COVID-19 Patients. *J. Med. Virol.* **2020**, *92*, 833–840. [CrossRef]
31. Hvitved-Jacobsen, T.; Vollertsen, J.; Nielsen, A.H. *Sewer Processes Microbial and Chemical Process Engineering of Sewer Networks*, 2nd ed.; Taylor & Francis: New York, NY, USA, 2013.
32. Ye, Y.; Ellenberg, R.M.; Graham, K.E.; Wigginton, K.R. Survivability, Partitioning, and Recovery of Enveloped Viruses in Untreated Municipal Wastewater. *Environ. Sci. Technol.* **2016**, *50*, 5077–5085. [CrossRef] [PubMed]
33. Gundy, P.M.; Gerba, C.P.; Pepper, I.L. Survival of Coronaviruses in Water and Wastewater. *Food Environ. Virol.* **2009**, *1*, 10–14. [CrossRef]
34. Nghiem, L.D.; Morgan, B.; Donner, E.; Short, M.D. The COVID-19 Pandemic: Considerations for the Waste and Wastewater Services Sector. *Case Stud. Chem. Environ. Eng.* **2020**, *1*, 100006. [CrossRef]
35. Naddeo, V.; Liu, H. Editorial Perspectives: 2019 Novel Coronavirus (SARS-CoV-2): What Is Its Fate in Urban Water Cycle and How Can the Water Research Community Respond? *Environ. Sci. Water Res. Technol.* **2020**, *6*, 1213–1216. [CrossRef]
36. Kostoglou, M.; Petala, M.; Karapantsios, T.; Dovas, C.; Roilides, E.; Metallidis, S.; Papa, A.; Stylianidis, E.; Papadopoulos, A.; Papaioannou, N. SARS-CoV-2 Adsorption on Suspended Solids along a Sewerage Network: Mathematical Model Formulation, Sensitivity Analysis, and Parametric Study. *Environ. Sci. Pollut. Res.* **2021**, *29*, 11304–11319. [CrossRef] [PubMed]
37. Hart, O.E.; Halden, R.U. Modeling Wastewater Temperature and Attenuation of Sewage-Borne Biomarkers Globally. *Water Res.* **2020**, *172*, 115473. [CrossRef]
38. Hart, O.E.; Halden, R.U. Computational Analysis of SARS-CoV-2/COVID-19 Surveillance by Wastewater-Based Epidemiology Locally and Globally: Feasibility, Economy, Opportunities and Challenges. *Sci. Total Environ.* **2020**, *730*, 138875. [CrossRef] [PubMed]
39. Ahmed, W.; Bertsch, P.M.; Bibby, K.; Haramoto, E.; Hewitt, J.; Huygens, F.; Gyawali, P.; Korajkic, A.; Riddell, S.; Sherchan, S.P.; et al. Decay of SARS-CoV-2 and Surrogate Murine Hepatitis Virus RNA in Untreated Wastewater to Inform Application in Wastewater-Based Epidemiology. *Environ. Res.* **2020**, *191*, 110092. [CrossRef]

40. Bivins, A.; Greaves, J.; Fischer, R.; Yinda, K.C.; Ahmed, W.; Kitajima, M.; Munster, V.J.; Bibby, K. Persistence of SARS-CoV-2 in Water and Wastewater. *Environ. Sci. Technol. Lett.* **2020**, *7*, 937–942. [CrossRef]
41. Hokajärvi, A.M.; Rytkönen, A.; Tiwari, A.; Kauppinen, A.; Oikarinen, S.; Lehto, K.M.; Kankaanpää, A.; Gunnar, T.; Al-Hello, H.; Blomqvist, S.; et al. The Detection and Stability of the SARS-CoV-2 RNA Biomarkers in Wastewater Influent in Helsinki, Finland. *Sci. Total Environ.* **2021**, *770*, 145274. [CrossRef]
42. Yang, S.; Dong, Q.; Li, S.; Cheng, Z.; Kang, X.; Ren, D.; Xu, C.; Zhou, X.; Liang, P.; Sun, L.; et al. Persistence of SARS-CoV-2 RNA in Wastewater after the End of the COVID-19 Epidemics. *J. Hazard. Mater.* **2022**, *429*, 128358. [CrossRef] [PubMed]
43. Katsifarakis, K.L.; Karpouzos, D.K. Genetic Algorithms and Water Resources Management: An Established, yet Evolving Relationship. In *Hydrology, Hydraulics and Water Resources Management*; WIT Press: Billerica, MA, USA, 2012; Volume 56, pp. 7–37, ISBN 0-932955-87-8.
44. Ostfeld, A.; Uber, J.G.; Salomons, E.; Berry, J.W.; Hart, W.E.; Phillips, C.A.; Watson, J.-P.; Dorini, G.; Jonkergouw, P.; Kapelan, Z.; et al. The Battle of the Water Sensor Networks (BWSN): A Design Challenge for Engineers and Algorithms. *J. Water Resour. Plan. Manag.* **2008**, *134*, 556–568. [CrossRef]
45. Anagnostopoulou, E. Optimal Design of Quality Sensors Placement in Water Distribution Systems. Master's Thesis, National Technical University of Athens, Athens, Greece, 2015.
46. Brentan, B.; Carpitella, S.; Barros, D.; Meirelles, G.; Certa, A.; Izquierdo, J. Water Quality Sensor Placement: A Multi-Objective and Multi-Criteria Approach. *Water Resour. Manag.* **2021**, *35*, 225–241. [CrossRef]
47. Jafari, H.; Nazif, S.; Rajaee, T. A Multi-Objective Optimization Method Based on NSGA-III for Water Quality Sensor Placement with the Aim of Reducing Potential Contamination of Important Nodes. *Water Supply* **2022**, *22*, 928–944. [CrossRef]
48. Banik, B.; Alfonso, L.; Di Cristo, C.; Leopardi, A. Greedy Algorithms for Sensor Location in Sewer Systems. *Water* **2017**, *9*, 856. [CrossRef]
49. Banik, B.K.; Alfonso, L.; Di Cristo, C.; Leopardi, A.; Mynett, A. Evaluation of Different Formulations to Optimally Locate Sensors in Sewer Systems. *J. Water Resour. Plann. Manag.* **2017**, *143*, 04017026. [CrossRef]
50. Banik, B.K.; Alfonso, L.; Torres, A.S.; Mynett, A.; Di Cristo, C.; Leopardi, A. Optimal Placement of Water Quality Monitoring Stations in Sewer Systems: An Information Theory Approach. *Procedia Eng.* **2015**, *119*, 1308–1317. [CrossRef]
51. Lee, J.H. Determination of Optimal Water Quality Monitoring Points in Sewer Systems Using Entropy Theory. *Entropy* **2013**, *15*, 3419–3434. [CrossRef]
52. Alfonso, L.; He, L.; Lobbrecht, A.; Price, R. Information Theory Applied to Evaluate the Discharge Monitoring Network of the Magdalena River. *J. Hydroinform.* **2013**, *15*, 211–228. [CrossRef]
53. Psarrou, E.; Tsoukalas, I.; Makropoulos, C. A Monte-Carlo-Based Method for the Optimal Placement and Operation Scheduling of Sewer Mining Units in Urban Wastewater Networks. *Water* **2018**, *10*, 200. [CrossRef]
54. Domokos, E.; Sebestyén, V.; Somogyi, V.; Trájer, A.J.; Gerencsér-Berta, R.; Horváth, B.O.; Tóth, E.G.; Jakab, F.; Kemenesi, G.; Abonyi, J. Identification of Sampling Points for the Detection of SARS-CoV-2 in the Sewage System. *Sustain. Cities Soc.* **2021**, *76*, 103422. [CrossRef]
55. Rossman, L.A. *Storm Water Management Model User's Manual Version 5.1*; U.S. Environmental Protection Agency (EPA): Cincinnaty, OH, USA, 2015.
56. Lowe, S.A. Sanitary Sewer Design Using EPA Storm Water Management Model (SWMM). *Comput. Appl. Eng. Educ.* **2010**, *18*, 203–212. [CrossRef]
57. Rossman, L.A.; Huber, W.C. *Storm Water Management Model Reference Manual Vollume III—Water Quality*; U.S. Environmental Protection Agency (EPA): Cincinnaty, OH, USA, 2016.
58. Li, X.; Zhang, S.; Shi, J.; Luby, S.P.; Jiang, G. Uncertainties in Estimating SARS-CoV-2 Prevalence by Wastewater-Based Epidemiology. *Chem. Eng. J.* **2021**, *415*, 129039. [CrossRef] [PubMed]
59. McDonnell, B.; Ratliff, K.; Tryby, M.; Wu, J.; Mullapudi, A. PySWMM: The Python Interface to Stormwater Management Model (SWMM). *J. Open Source Softw.* **2020**, *5*, 2292. [CrossRef] [PubMed]
60. Deb, K.; Pratap, A.; Agarwal, S.; Meyarivan, T. A Fast and Elitist Multiobjective Genetic Algorithm: NSGA-II. *IEEE Trans. Evol. Comput.* **2002**, *6*, 182–197. [CrossRef]
61. Blank, J.; Deb, K. Pymoo: Multi-Objective Optimization in Python. *IEEE Access* **2020**, *8*, 89497–89509. [CrossRef]
62. IMEdD LAB. Available online: https://lab.imedd.org/covid19/?lang=en (accessed on 8 May 2023).
63. Pecson, B.M.; Darby, E.; Haas, C.N.; Amha, Y.M.; Bartolo, M.; Danielson, R.; Dearborn, Y.; Di Giovanni, G.; Ferguson, C.; Fevig, S.; et al. Reproducibility and Sensitivity of 36 Methods to Quantify the SARS-CoV-2 Genetic Signal in Raw Wastewater: Findings from an Interlaboratory Methods Evaluation in the U.S. *Environ. Sci. Water Res. Technol.* **2021**, *7*, 504–520. [CrossRef]
64. Tchobanoglous, G.; Burton, F.L.; Stensel, D.H. *Wastewater Engineering: Treatment and Reuse*, 4th ed.; Metcalf & Eddy Inc.: Wakefield, MA, USA, 2003.
65. Guo, Y.; Liu, Y.; Gao, S.; Zhou, X.; Sivakumar, M.; Jiang, G. Effects of Temperature and Water Types on the Decay of Coronavirus: A Review. *Water* **2023**, *15*, 1051. [CrossRef]
66. Hwang, C.L.; Lai, Y.J.; Liu, T.Y. A New Approach for Multiple Objective Decision Making. *Comput. Oper. Res.* **1993**, *20*, 889–899. [CrossRef]
67. Wang, Z.; Rangaiah, G.P. Application and Analysis of Methods for Selecting an Optimal Solution from the Pareto-Optimal Front Obtained by Multiobjective Optimization. *Ind. Eng. Chem. Res.* **2017**, *56*, 560–574. [CrossRef]

68. Zionts, S.; Wallenius, J. An Interactive Multiple Objective Linear Programming Method for a Class of Underlying Nonlinear Utility Functions. *Manag. Sci.* **1983**, *29*, 519–529. [CrossRef]
69. Vallejo, J.A.; Trigo-Tasende, N.; Rumbo-Feal, S.; Conde-Pérez, K.; López-Oriona, Á.; Barbeito, I.; Vaamonde, M.; Tarrío-Saavedra, J.; Reif, R.; Ladra, S.; et al. Modeling the Number of People Infected with SARS-CoV-2 from Wastewater Viral Load in Northwest Spain. *Sci. Total Environ.* **2022**, *811*, 152334. [CrossRef] [PubMed]